Available online at www.sciencedirect.com
ScienceDirect
Journal of Magnetic Resonance 187 (2007) 352–356
JMR Journal of Magnetic Resonance
www.elsevier.com/locate/jmr

Communication

Determination of chemical shift anisotropies of unresolved carbonyl sites by C-α detection under magic-angle spinning

Yun Mou, Peng-Huan Chen, Hsin-Wen Lee, Jerry C.C. Chan *

Department of Chemistry, National Taiwan University, No. 1, Section 4, Roosevelt Road, Taipei, Taiwan

Received 7 February 2007; revised 3 April 2007
Available online 23 May 2007

Abstract

We demonstrate that the static powder pattern line shape of chemical shift anisotropy (CSA) can be obtained for unresolved carbonyl sites of polypeptides under magic-angle spinning. The CSA interaction is first recoupled at the carbonyl site. The phase factors associated with the CSA recoupling are then transferred to the adjacent α carbon by an isotropic polarization transfer based on scalar spin–spin coupling. Because α carbons of polypeptides are usually better resolved, we can then obtain the CSA static powder pattern line shapes of the carbonyl sites after Fourier transformation in the second dimension. We validate our approach experimentally by measurements on [U–^{13}C, ^{15}N]-L-alanine, [U–^{13}C, ^{15}N]-L-valine and prion fibrils with uniform ^{13}C and ^{15}N labels on selected residues.

Keywords: SSNMR; CSA; TOBSY; ROCSA; Polypeptides; Recouplings; Fibrils

1. Introduction

Solid-state nuclear magnetic resonance (SSNMR) has proven to be an indispensable technique for the structural elucidation of non-crystalline biological solids [1,2]. Under magic-angle spinning (MAS), which is a standard method for obtaining high resolution spectra in SSNMR, there are many different pulse sequences developed for characterizing the anisotropic interactions in the second dimension [3]. Anisotropic interactions such as chemical shift anisotropy (CSA) have a strong dependence on molecular structures. It is well known that CSA data could provide valuable structural information in polypeptides [4–8]. Various pulse sequences have been developed for the recoupling of the CSA interaction [9–13], from which one can obtain a static powder pattern line shape under MAS [9,11,13]. In particular, the pulse sequence ROCSA (recoupling of CSA) has the virtue that homonuclear dipole–dipole interaction is actively suppressed by the pulse symmetry [9] and therefore ROCSA has been incorporated in spin interaction tensor correlation experiments for the determination of backbone torsion angles in uniformly ^{13}C labeled systems [14]. In brief, the chemical shift tensor of the carbonyl carbon (C′) and the C_α–H_α dipolar tensor are correlated to determine the ψ angle. For polypeptides with inherent structural disorders, however, the ^{13}C signals in the carbonyl region are usually poorly resolved. Therefore, the characterization of the C′ CSA, which is required for data analysis, will become very difficult if more than one carbonyl carbons are ^{13}C labeled.

In this contribution, we develop a simple strategy to obtain site-resolved C′ CSA patterns under MAS. Because the C_α signals of polypeptides are usually better resolved than the C′ signals, one may transfer the C′ CSA patterns to the neighboring C_α for subsequent detection. To avoid any distortion of the C′ CSA pattern, it is necessary to employ isotropic scalar spin–spin coupling for the homonuclear polarization transfer [15–19]. The major disadvantage of dipolar-based polarization transfer is that the C′–C_α dipolar interaction will modulate the C′ CSA pattern and such modulation may be dependent on the relative orientation of the C′ and C_α chemical shift tensors, which is usually unknown. Our strategy is to recouple the

* Corresponding author. Fax: +886 2 2363 6359.
E-mail address: chanjcc@ntu.edu.tw (J.C.C. Chan).

1090-7807/$ - see front matter © 2007 Elsevier Inc. All rights reserved.
doi:10.1016/j.jmr.2007.05.002

C′ CSA by ROCSA [9] and then transfer the pattern to C_α for detection by the pulse sequence R-TOBSY [18]. We demonstrate our "C_α-detection" scheme experimentally by measurements on [U–^{13}C, ^{15}N]-L-alanine, [U–^{13}C, ^{15}N]-L-valine and prion fibrils with uniform ^{13}C and ^{15}N labels on selected residues.

2. Experimental method

2.1. Sample preparation

Uniformly ^{13}C- and ^{15}N-labeled L-alanine and L-valine were used as received from Cambridge Isotopes Laboratories. The peptides corresponding to a fragment of Syrian hamster prion protein ($SHPrP_{109–122}$), with the sequence MKHMAGAAAAGAVV, were synthesized on a PS3 (Rainin) peptide synthesizer by 9-fluorenylmethoxycarbonyl (FMOC) chemistry, using a Rink amide resin (0.6 mequiv/g substitution level; Novabiochem). The peptides were uniformly ^{13}C and ^{15}N-labeled at the positions of Ala113, Gly119 and Val122. The crude material was purified by high-performance liquid chromatography at 50 °C, using a water/acetonitrile gradient with 0.1% TFA and a preparative scale Vydac C18 reverse-phase column. Fibril samples were formed by dissolution of purified $SHPrP_{109–122}$ at a peptide concentration of 745 μM in 100 mM NaCl and 20 mM *N*-cyclohexyl-2-aminoethanesulfonic acid (Hepes buffer, pH 7.4), with addition of 0.01% NaN_3. Dissolution was assisted by sonication. Fibrils formed after incubation at 37 °C for one day, appearing as a visible precipitate. Before NMR measurements, the salts were removed by repeated dissolution in D.I. water and centrifuge for three times, and then lyophilized.

2.2. Solid-state NMR

All NMR experiments were carried out at ^{13}C and ^{1}H frequencies of 75.5 and 300.1 MHz, respectively, on a Bruker DSX300 NMR spectrometer equipped with a commercial 2.5 mm probe. ^{13}C chemical shifts were referenced to TMS using adamantane as the secondary standard. The spectra were measured at a spinning frequency of 25 kHz. The MAS frequency variation was limited to ±5 Hz using a commercial pneumatic control unit. Each sample was confined in the middle one-half of the rotor volume using Teflon spacers. The recycle delay was set to 2 s. During the cross-polarization contact time (1.5 ms), the ^{1}H nutation frequency was set to 50 kHz and that of ^{13}C was ramped through the Hartmann–Hahn matching condition [20,21]. The durations of the Gaussian selective pulse and the z-filter were set to 0.2 and 10 ms, respectively. Continuous-wave (40 kHz) and XiX [22] proton decouplings (100 kHz) were applied during the CSA recoupling and the acquisition periods, respectively. The ^{13}C nutation frequencies were set to 100 and 125 kHz for the ROCSA and for the R-TOBSY pulse blocks, as required by the pulse symmetries [9,23,24]. The transmitter frequency was centered on the C′ signal during the ROCSA recoupling period, and that during the R-TOBSY transfer period was set near the middle of the C′ and C_α signals, and then optimized carefully to give the maximum polarization transfer. The R-TOBSY mixing time was set to 7.68 ms. For L-alanine and L-valine, two transients together with a two-step phase cycling for spin-temperature inversion were accumulated for each t_1 increment, and a total of 26 increments were done at steps of 80 μs. For the fibril sample, 512 transients were accumulated for each t_1 increment. Spectral artifacts are suppressed by inverting the phase of the ^{13}C $\pi/2$ pulse right after the ROCSA pulse block and alternating addition and subtraction of FID signals. Together with CYCLOPS [25] and the spin-temperature inversion, the phase cycling scheme has a total of 16 steps. For all the two-dimensional spectra, Gaussian window functions of 200 and 25 Hz were applied in the t_1 and t_2 dimensions, respectively, before the Fourier transformation. For the measurements of the fibril sample, a stream of dry cooling air at −11 °C (800 L/h) was used to keep the sample temperature at around 30 °C, calibrated by measurements on lead (II) nitrate.

2.3. Numerical simulations

Numerical simulations used to compare with experimental data were carried out using SIMPSON (version 1.1.0) [26]. For our simulations, the maximum time step over which the Hamiltonian is approximated to be time-independent was set to 1 μs. Typically, a powder averaging scheme containing 100 REPULSION angles (α and β) [27] and 18 γ angles was chosen. Relaxation effects were ignored. The simulations shown in Fig. 2 were done on a three-spin (C', C_α, C_β) system where the initial density operator contains the polarization from C′ only. The ^{13}C′ CSA and all other structural parameters of L-alanine were obtained from the literature [20,21]. All the pulse durations and the rf fields were matched to the experimental conditions.

The principal components of the chemical shift tensor of the model compounds and the fibril sample were obtained by fitting the experimental spectrum with numerical simulations (Figs. 3 and 5). The simulations were done on a one-spin system under the influence of the ROCSA pulse sequence. The variables being optimized were the chemical shift anisotropy and the asymmetry parameter. Other simulation parameters were matched to the experimental conditions. The non-linear least-square fitting procedure was done by the MINUIT package incorporated in SIMPSON package [27].

3. Results and discussion

Fig. 1 shows the pulse sequence we developed for the C_α-detection scheme. Taking the advantage that the carbonyl region and the aliphatic region are well separated

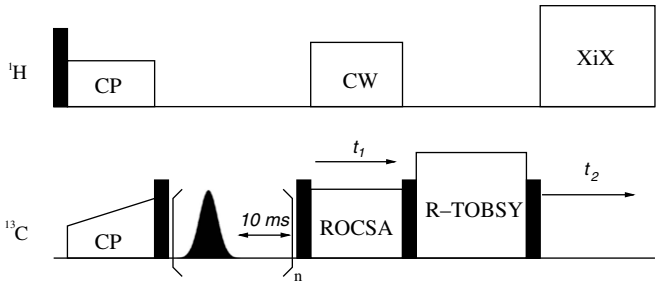

Fig. 1. Pulse sequence of the C_α-detection scheme of C′ CSA patterns. The filled rectangles denote π/2 pulses. The Gaussian pulse positioned in the aliphatic region has a flip angle of π/2. Typically, *n* is set to 10 for a clean suppression of the aliphatic signals.

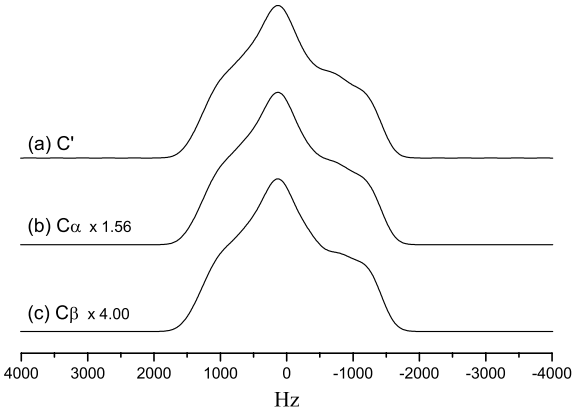

Fig. 2. Simulated spectra of the C′ CSA pattern of L-alanine. (a) Direct detection. (b) C_α-detection. (c) C_β-detection. The spectra of (a) and (b) were scaled up by factors of 1.56 and 4.00, respectively, to alleviate the effect of different efficiencies in the polarization transfer. Simulations were carried out on a three-spin system (C′, C_α, C_β).

spectrally, it is possible to selectively preserve the C′ polarization for the subsequent CSA recoupling. After the cross-polarization, a hard pulse in the ^{13}C channel was used to flip all the magnetizations onto the *z*-axis. A soft Gaussian π/2 pulse positioned at the aliphatic region was applied to excite the C_α and C_β signals, which were subsequently dephased by the z-filter. The soft-pulse-z-filter cycle was repeated for several times to obtain a clean suppression of the aliphatic carbon signals. After that, the C′ magnetization was excited by another hard π/2 pulse and then evolved under the influence of the average Hamiltonian prepared by ROCSA, which is identical to the static CSA Hamiltonian except for a scaling factor [9]. As required for quadrature detection in the t_1 dimension [25], the *x* or *y*-components of the C′ transverse magnetization immediately after the t_1 evolution was flipped onto the *z*-axis by a hard π/2 pulse, which was then transferred to the neighboring C_α via the R-TOBSY recoupling sequence, followed by a reading π/2 pulse. The resolution of the C_α signals is then exploited to characterize the CSA patterns of those overlapping C′ signals.

To investigate the usefulness of our approach, we carried out numerical simulations by solving the Liouville–von Neumann equation numerically. Our calculations were done on a three-spin (C′, C_α and C_β) system at 7.05 T, on the basis of the NMR [28] and geometry [29] parameters of L-alanine. Fig. 2a shows the regular ROCSA pattern of the C′ site of L-alanine. The corresponding C′ CSA pattern detected by C_α is illustrated in Fig. 2b. As expected, the two CSA patterns are essentially identical because the ^{13}C homonuclear polarization transfer provided by R-TOBSY is isotropic. As the average Hamiltonian created by R-TOBSY has a flip-flop term, a relay polarization transfer from C′ to C_β is also observed (Fig. 2c). Dictated by the transfer efficiency of R-TOBSY, the signal intensities are c.a. 64 and 25% for Fig. 2b and c, respectively, relative to that of Fig. 2a.

Fig. 3 shows the C_α-detected CSA patterns measured for C′ carbons of [U–^{13}C, ^{15}N]-L-alanine and [U–^{13}C, ^{15}N]-L-valine. The simulated spectra are non-linear least-squares fit to the experimental ones. Together with the isotropic chemical shifts obtained in the MAS spectra, the principal components of the chemical shift tensors were extracted and summarized in Table 1, where we find a good agreement between the fitting results and the literature data.

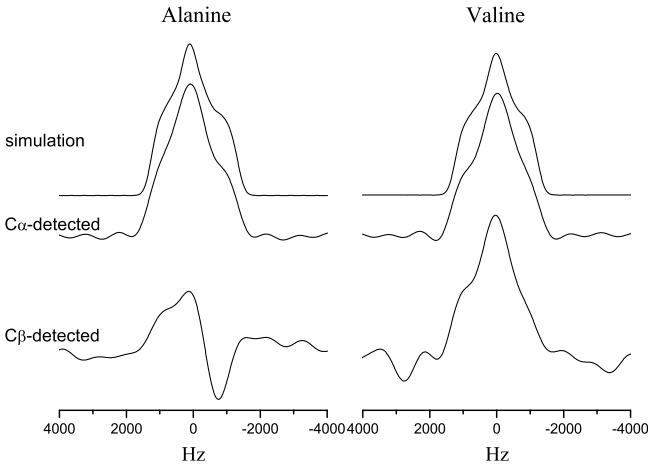

Fig. 3. Experimental and the best-fit simulated spectra of [U–^{13}C, ^{15}N]-L-alanine and [U–^{13}C, ^{15}N]-L-valine. Simulations correspond to the evolution of a one-spin system under the ROCSA sequence. The only variables are the chemical shift anisotropy and the asymmetry parameter. A Gaussian window function of 400 Hz was applied to the simulated spectrum before the Fourier transformation.

Table 1
The principal components of the C′ chemical shift tensors obtained for model compounds and the fibril sample

	Detected site	Experimental data (ppm)			Literature data (ppm)			Reference
		δ_{11}	δ_{22}	δ_{33}	δ_{11}	δ_{22}	δ_{33}	
L-Alanine	C_α	242	182	106	239	184	106	[32]
L-Valine	C_α	241	176	111	244	176	108	[32]
	C_β	243	176	108				
Ala113	C_α	244	186	95				—
Gly119	C_α	243	180	97				—
Val122	C_α	241	168	96				—

The $SHPrP_{109–122}$ fibril sample was uniformly ^{13}C- and ^{15}N-labeled at the residues Ala113, Gly119 and Val122.

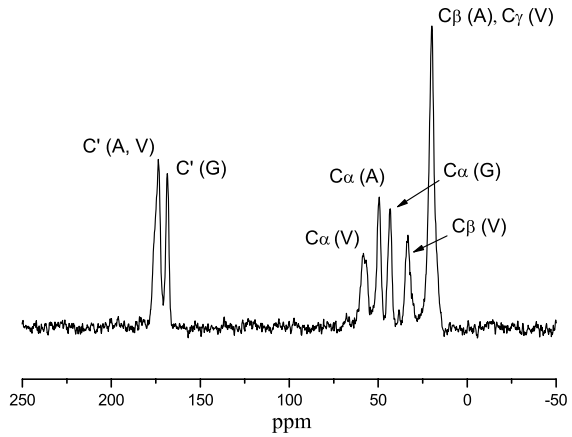

Fig. 4. $^{13}C\{^{1}H\}$ CPMAS spectrum of the $SHPrP_{109–122}$ fibril sample.

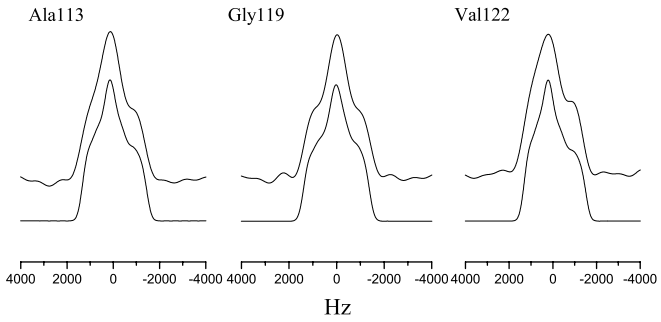

Fig. 5. C_α-detected C′ CSA patterns of the $SHPrP_{109–122}$ fibril sample. The upper and lower traces correspond to the experimental and the simulated spectra, respectively. Other conditions are identical to those described in Fig. 3.

As demonstrated by numerical simulations, R-TOBSY also allows the C_β detection of the C′ CSA pattern (Fig. 3). In spite of the lower signal-to-noise ratio, the C_β-detected pattern resembles closely to that detected by C_α for [U–^{13}C, ^{15}N]-L-valine. On the other hand, the C_β-detected C′ CSA pattern of [U–^{13}C, ^{15}N]-L-alanine is seriously distorted. The distortion is most likely due to the interference of the spin–lattice relaxation during the R-TOBSY period, because the spin–lattice relaxation times of the C_β signals were found to be approximately 790 and 80 ms for L-valine and L-alanine, respectively. On the other hand, the spin–lattice relaxation time of the C_α of L-alanine was found to be approximately 400 ms.

To illustrate the real applications of the C_α-detection scheme, we studied the prion fibrils formed by $SHPrP_{109–122}$ [30,31], in which the residues Ala113, Gly119 and Val122 are uniformly ^{13}C- and ^{15}N-labeled. Fig. 4 shows the $^{13}C\{^{1}H\}$ CPMAS spectrum, in which the assignments were made by ^{13}C–^{13}C correlation spectroscopy (data not shown). The C′ signals of Ala113 and Val122 are overlapping but their C_α signals are well resolved. Fig. 5 shows the C_α-detected CSA patterns. Together with the isotropic chemical shifts determined in Fig. 4, the principal components of the C′ chemical shift tensors of Ala113, Gly119 and Val122 were extracted (Table 1). The minor distortion of the C′ CSA pattern of Val122 may be attributed to the structural disorder at the C terminal of the polypeptide. On the basis of the experimental data shown in Figs. 3 and 5, the C_α-detection scheme for C′ CSA pattern is a robust one, as long as the spin–lattice relaxation times of the C′ and C_α signals are significantly longer than the polarization transfer period. The effects of other experimental imperfections such as off-resonance effect and rf inhomogeneity are immaterial in our case, as demonstrated in the studies of the R-TOBSY and ROCSA sequences [9,23].

Very recently, Nishiyama et al. have developed a method to characterize the C′ CSA of overlapping signals [10]. Their method requires the condition of off-magic-angle spinning and therefore may not be optimized for the characterization of C′ CSA of polypeptides with more than two uniformly labeled residues. Our method, on the other hand, solely depends on the resolution of the C_α signals and could be applied to polypeptides with multiple uniformly labeled residues.

Acknowledgment

This work was supported by grants from the National Science Council.

References

[1] R. Tycko, Applications of solid state NMR to the structural characterization of amyloid fibrils: methods and results, Prog. Nucl. Magn. Reson. Spectrosc. 42 (2003) 53–68.
[2] M. Baldus, Correlation experiments for assignment and structure elucidation of immobilized polypeptides under magic angle spinning, Prog. Nucl. Magn. Reson. Spectrosc. 41 (2002) 1–47.
[3] I. Schnell, Dipolar recoupling in fast-MAS solid-state NMR spectroscopy, Prog. Nucl. Magn. Reson. Spectrosc. 45 (2004) 145–207.
[4] F.J. Blanco, R. Tycko, Determination of polypeptide backbone dihedral angles in solid state NMR by double quantum C-13 chemical shift anisotropy measurements, J. Magn. Reson. 149 (2001) 131–138.
[5] M. Hong, Solid-state NMR determination of C-13 alpha chemical shift anisotropies for the identification of protein secondary structure, J. Am. Chem. Soc. 122 (2000) 3762–3770.
[6] R. Witter, U. Sternberg, A.S. Ulrich, NMR chemical shift powder pattern recoupling at high spinning speed and theoretical tensor evaluation applied to silk fibroin, J. Am. Chem. Soc. 128 (2006) 2236–2243.
[7] S. Wi, H.H. Sun, E. Oldfield, M. Hong, Solid-state NMR and quantum chemical investigations of C-13(alpha) shielding tensor magnitudes and orientations in peptides: determining phi and psi torsion angles, J. Am. Chem. Soc. 127 (2005) 6451–6458.
[8] H.H. Sun, L.K. Sanders, E. Oldfield, Carbon-13 NMR shielding in the twenty common amino acids: comparisons with experimental results in proteins, J. Am. Chem. Soc. 124 (2002) 5486–5495.
[9] J.C.C. Chan, R. Tycko, Recoupling of chemical shift anisotropies in solid-state NMR under high-speed magic-angle spinning and in uniformly C-13-labeled systems, J. Chem. Phys. 118 (2003) 8378–8389.
[10] Y. Nishiyama, T. Yamazaki, T. Terao, Development of modulated rf sequences for decoupling and recoupling of nuclear-spin interactions in sample-spinning solid-state NMR: application to chemical-shift anisotropy determination, J. Chem. Phys. 124 (2006). Art. No. 064304.

[11] S.F. Liu, J.D. Mao, K. Schmidt-Rohr, A robust technique for two-dimensional separation of undistorted chemical-shift anisotropy powder patterns in magic-angle-spinning NMR, J. Magn. Reson. 155 (2002) 15–28.
[12] R.M. Orr, M.J. Duer, Recoupling of chemical-shift anisotropy powder patterns in MAS NMR, J. Magn. Reson. 181 (2006) 1–8.
[13] R. Tycko, G. Dabbagh, P.A. Mirau, Determination of chemical-shift-anisotropy lineshapes in a two-dimensional magic-angle-spinning NMR experiment, J. Magn. Reson. 85 (1989) 265–274.
[14] J.C.C. Chan, R. Tycko, Solid-state NMR spectroscopy method for determination of the backbone torsion angle psi in peptides with isolated uniformly labeled residues, J. Am. Chem. Soc. 125 (2003) 11828–11829.
[15] E.H. Hardy, A. Detken, B.H. Meier, Fast-MAS total through-bond correlation spectroscopy using adiabatic pulses, J. Magn. Reson. 165 (2003) 208–218.
[16] M. Baldus, B.H. Meier, Total correlation spectroscopy in the solid state. The use of scalar couplings to determine the through-bond connectivity, J. Magn. Reson. A 121 (1996) 65–69.
[17] A.S.D. Heindrichs, H. Geen, C. Giordani, J.J. Titman, Improved scalar shift correlation NMR spectroscopy in solids, Chem. Phys. Lett. 335 (2001) 89–96.
[18] Y. Mou, J.C.H. Chao, J.C.C. Chan, Efficient spin–spin scalar coupling mediated C-13 homonuclear polarization transfer in biological solids without proton decoupling, Solid State Nucl. Magn. Reson. 29 (2006) 278–282.
[19] Y. Mou, J.C.C. Chan, Frequency selective polarization transfer based on multiple chemical shift precession, Chem. Phys. Lett. 419 (2006) 144–148.
[20] S. Hediger, B.H. Meier, N.D. Kurur, G. Bodenhausen, R.R. Ernst, NMR cross-polarization by adiabatic passage through the Hartmann–Hahn condition (Aphh), Chem. Phys. Lett. 223 (1994) 283–288.
[21] S. Hediger, B.H. Meier, R.R. Ernst, Adiabatic passage Hartmann–Hahn cross-polarization in NMR under magic-angle sample-spinning, Chem. Phys. Lett. 240 (1995) 449–456.
[22] A. Detken, E.H. Hardy, M. Ernst, B.H. Meier, Simple and efficient decoupling in magic-angle spinning solid-state NMR: the XiX scheme, Chem. Phys. Lett. 356 (2002) 298–304.
[23] J.C.C. Chan, G. Brunklaus, R sequences for the scalar-coupling mediated homonuclear correlation spectroscopy under fast magic-angle spinning, Chem. Phys. Lett. 349 (2001) 104–112.
[24] Y. Mou, Tim W.T. Tsai, J.C.C. Chan, Determination of the backbone torsion psi angle by tensor corelation of chemical shift anisotropy and heteronuclear dipole-dipole interaction, Solid State Nucl. Magn. Reson. 31 (2007) 72–81.
[25] R. Freeman, Spin Choreography: Basic Steps in High Resolution NMR, Oxford University Press, New York, 1998.
[26] M. Bak, J.T. Rasmussen, N.C. Nielsen, SIMPSON: a general simulation program for solid-state NMR spectroscopy, J. Magn. Reson. 147 (2000) 296–330.
[27] M. Bak, N.C. Nielsen, REPULSION, a novel approach to efficient powder averaging in solid-state NMR, J. Magn. Reson. 125 (1997) 132–139.
[28] A. Naito, S. Ganapathy, K. Akasaka, C.A. McDowell, Chemical shielding tensor and C-13–N-14 dipolar splitting in single-crystals of L-alanine, J. Chem. Phys. 74 (1981) 3190–3197.
[29] M.S. Lehmann, T.F. Koetzle, W.C. Hamilton, Precision neutron diffraction structure determination of protein and nucleic acid components. I. The crystal and molecular structure of the amino acid L-alanine, J. Am. Chem. Soc. 94 (1972) 2657–2660.
[30] M. Gasset, M.A. Baldwin, D.H. Lloyd, J.M. Gabriel, D.M. Holtzman, F. Cohen, R. Fletterick, S.B. Prusiner, Predicted alpha-helical regions of the prion protein when synthesized as peptides form amyloid, Proc. Natl. Acad. Sci. USA 89 (1992) 10940–10944.
[31] S.A. Petty, S.M. Decatur, Intersheet rearrangement of polypeptides during nucleation of beta-sheet aggregates, Proc. Natl. Acad. Sci. USA 102 (2005) 14272–14277.
[32] C.H. Ye, R.Q. Fu, J.Z. Hu, L. Hou, S.W. Ding, C-13 chemical-shift anisotropies of solid amino-acids, Magn. Reson. Chem. 31 (1993) 699–704.